ISSN 0005-1179 (print), ISSN 1608-3032 (online), Automation and Remote Control, 2026, Vol. 87, No. 7, pp. 572–584.

LINEAR SYSTEMS

An Approach to Finding Points Inside the Reachable Set for a Linear Discrete Large-Order Model with Time-Varying Parameters

V. I. Kruzhkov

Trapeznikov Institute of Control Sciences, Russian Academy of Sciences, Moscow, Russia
e-mail: kruzhkov@ipu.ru

Received June 6, 2025
Revised November 11, 2025
Accepted November 14, 2025

Abstract—A method is proposed for finding reachable values of the output vector, taking into account constraints on the input and output signals during the control process for linear discrete systems with variable parameters. The developed algorithm overcomes the computational limitations of traditional approaches when working with high-order models. The method is based on sequential analysis of the output vector components by reducing them to linear programming problems. Its application is demonstrated using the example of the Globus-M2 spherical tokamak plasma model, where the possibility of determining attainable plasma configurations under constraints on the control voltages and currents is shown.

Keywords: linear systems, digital systems, systems with variable parameters, reachability set, plasma, tokamak

DOI: 10.7868/S1608303226070027

1. INTRODUCTION

The problem of determining reachability sets (RS) for dynamical systems is central in control theory [1–3]. Classical approaches to determining the RS for systems with controls belonging to a given set, described in [1, 4–8], face significant computational difficulties when analyzing high-order system models typical of modern applications, including plasma control systems in tokamaks. The main limitations of traditional methods stem from the exponential growth of computational complexity, the need to construct convex hulls in high-dimensional spaces, limited applicability to systems with variable parameters and constraints on output signals, which makes accurate determination of the RS computationally challenging for high-order plant models. This paper proposes an iterative approach that enables efficient finding of points inside the RS for systems with tens of state variables, takes into account parametric changes in the model, and obtains practically useful estimates for engineering applications.

The method for computing the reachability set in the problem formulation described below in (6) was proposed in [4–6], where it was shown that using dynamic programming a multi-step estimate of the RS can be reduced to a recurrent computation of one-step estimates. The latter, in turn, reduce to constructing the convex hull of a set of points in an n-dimensional space corresponding to the dimension of the state vector.

In [4–6], modifications of the simplex method are used to construct the convex hull. An alternative approach is based on space partitioning, similar to the quicksort algorithm [9]. Although this method has no fundamental restrictions on the class of models, it requires significant computational resources [4] when the state vector dimension is high. This is because the number of hyperfaces of a d-polytope with N vertices can reach [9, 10]:

$$F(d,N) = \begin{cases} \dfrac{2N}{d} C_{N-d/2-1}^{d/2-1}, & \text{for even } d, \\ 2C_{N-\lfloor d/2 \rfloor -1}^{\lfloor d/2 \rfloor -1}, & \text{for odd } d, \end{cases} \tag{1}$$

where $\lfloor \cdot \rfloor$ denotes the floor function, $C_n^k = \frac{n!}{k!(n-k)!}$ is the binomial coefficient. Thus, $F(d,N) = O(N^{\lfloor d/2 \rfloor})$, which indicates an exponential growth in complexity as the number of vertices increases.

The method of [1, 7, 8] is based on approximating the RS by sets of simple structure, namely ellipsoids. Such a description is efficient for small phase space dimensions ($n = 2, 3$), but for large dimensions this method is laborious and provides a very incomplete representation of the reachable set [1, 7, 11].

This computational complexity makes it impractical to apply the algorithm to models with tens of state variables, including tokamak models and their control systems [12–14]. In this paper, an approach is proposed that overcomes this limitation by sequentially estimating the RS along the components of the output vector using the simplex method for solving linear programming problems [15–17]. Although the simplex method has exponential complexity in the worst case, in practice it exhibits polynomial convergence on average [17]. The price for increased efficiency is obtaining not full information about the RS but only its cross-sections. However, this method allows finding reachable points under given control constraints.

In [18, 19] a different approach is applied, consisting of two ideas: estimating the reachability set in steady-state and dividing the multidimensional RS into upper and lower estimates. The methodology based on considering the steady state is applicable to stationary and quasi-stationary plants, in which the characteristic time of parameter variation is orders of magnitude higher than the characteristic time of transients. The approach of dividing the RS into upper and lower estimates is illustrative and efficient for multidimensional plants. The upper estimate of the RS is described around the real reachability set, and the lower estimate is inscribed inside it. Thus, all points inside the lower estimate are reachable, and no points outside the upper estimate are reachable. However, in the case of strong coupling between channels and asymmetric constraints on the control and/or initial states, such an approach leads to an expansion of the "gray area" between the upper and lower estimates for points about which it is impossible to say whether they are reachable or not. This is illustrated in Section 4 in Fig. 1.

Further, Section 2 presents the problem statement. Section 3 describes preliminary computations allowing one to obtain the matrix relationship between the system outputs, given the inputs and initial conditions. Section 4 provides a sequential upper estimate of the reachability set based on previous results and compares the sequential estimate with the upper and lower estimates from [18, 19]. In Section 5 the sequential estimate is applied to a model example, showing that the results agree with those obtained by the method of [4–6]. Section 6 finds the dynamics of reachability sets with respect to plasma shape for models of the Globus-M2 tokamak with variable parameters and verifies these results in numerical experiments. The Conclusion summarizes the main results of the work.

2. PROBLEM STATEMENT

Consider a discrete-time plant model in the state space of dimension n, with p inputs and two groups of outputs of dimensions m and r, with variable parameters:

$$\begin{aligned} x_{k+1} &= A_k x_k + B_k u_k, \\ y_k &= C_k x_k + D_k u_k, \\ \tilde{y}_k &= \tilde{C}_k x_k + \tilde{D}_k u_k, \end{aligned} \tag{2}$$

where $k \in [1, T]$, the matrices A_k, B_k, C_k, $\tilde{C}_k$, D_k, $\tilde{D}_k$ have appropriate dimensions, x_k is the state vector, u_k is the control vector, y_k and $\tilde{y}_k$ are output vectors. The following constraints are considered:

- on the initial state vector

$$X_1 = \{x : x \in \mathbb{R}^n, x^{(i)}_{\min} \leqslant x^{(i)} \leqslant x^{(i)}_{\max}, i \in [1, n]\},\ x_1 \in X_1; \tag{3}$$

- on the controls at each step

$$P = \{u : u \in \mathbb{R}^p, u^{(i)}_{\min} \leqslant u^{(i)} \leqslant u^{(i)}_{\max}, i \in [1, p]\},\ u_k \in P; \tag{4}$$

- on the second group of output vectors at each step

$$F = \{\tilde{y} : \tilde{y} \in \mathbb{R}^r, \tilde{y}^{(i)}_{\min} \leqslant \tilde{y}^{(i)} \leqslant \tilde{y}^{(i)}_{\max}, i \in [1, r]\},\ \tilde{y}_k \in F. \tag{5}$$

The superscript $x^{(i)}$ denotes the i-th element of the vector x.

By the state reachability set in system (2) with constraints (3), (4), (5) at the end of the Tth step, similarly to [2–4], we shall call the set

$$\begin{aligned} &G(x_{\min}, x_{\max}, u_{\min}, u_{\max}, \tilde{y}_{\min}, \tilde{y}_{\max}, T) = \{x_T : x_T \in \mathbb{R}^n \quad \forall k \in [1, T-1], \\ &x_{k+1} = A_k x_k + B_k u_k, \tilde{y}_k = \tilde{C}_k x_k + \tilde{D}_k u_k, x_1 \in X_1, u_k \in P, \tilde{y} \in F\}. \end{aligned} \tag{6}$$

By the output reachability set we shall call the set

$$\begin{aligned} &Y(x_{\min}, x_{\max}, u_{\min}, u_{\max}, \tilde{y}_{\min}, \tilde{y}_{\max}, T) = \{y_T : y_T \in \mathbb{R}^m, \\ &y_T = C_T x_T + D_T u_T, x_T \in G(x_{\min}, x_{\max}, u_{\min}, u_{\max}, \tilde{y}_{\min}, \tilde{y}_{\max}, T), u_T \in P\}. \end{aligned} \tag{7}$$

In [4] it is shown that set (6) under constraints of the form (3), (4) is a convex polyhedron with a finite number of vertices. By similar reasoning one can show that (7) under constraints of the same type is also a convex polyhedron with a finite number of vertices.

3. DERIVATION OF INPUT-OUTPUT MATRIX RELATION

Let us find the matrix relation between the initial state vector x_1, the control actions u_i and the state vector at the kth step for model (2). Since $x_{k+1} = A_k x_k + B_k u_k$, the state vector can be computed according to the formula:

$$\begin{aligned} &x_2 = A_1 x_1 + B_1 u_1, \\ &x_3 = A_2 x_2 + B_2 u_2 = A_2(A_1 x_1 + B_1 u_1) + B_2 u_2, \\ &\quad \dots \\ &x_k = A_{k-1} \cdots A_1 x_1 + A_{k-1} \cdots A_2 B_1 u_1 + A_{k-1} \cdots A_3 B_2 u_2 + \cdots + B_{k-1} u_{k-1}. \end{aligned} \tag{8}$$

Using the relation $y_k = C_k x_k + D_k u_k$, we obtain the output vector values

$$\begin{aligned} &y_1 = C_1 x_1 + D_1 u_1, \\ &y_2 = C_2 x_2 + D_2 u_2 = C_2(A_1 x_1 + B_1 u_1) + D_2 u_2, \\ &\quad \dots \\ &y_k = C_k(A_{k-1} \cdots A_1 x_1 + A_{k-1} \cdots A_2 B_1 u_1 + \cdots + B_{k-1} u_{k-1}) + D_k u_k. \end{aligned} \tag{9}$$

Combining the vectors of initial values and control signals at all steps up to the kth inclusive into a column vector

$$U_k = [x_1^\top, u_1^\top, \dots, u_k^\top]^\top \tag{10}$$

and introducing the notation

$$M_k = [C_kA_{k-1}\cdots A_1, C_kA_{k-1}\cdots A_2B_1, C_kA_{k-1}\cdots A_3B_2, \ldots, C_kB_{k-1}, D_k], \tag{11}$$

we obtain the matrix relation between all control signals, the initial state, and the output vector at the kth step:

$$y_k = M_kU_k, \tag{12}$$

where $M_k \in \mathbb{R}^{m\times(kp+n)}$, $U_k \in \mathbb{R}^{(kp+n)}$. Similarly, we find the values of the second group of output signals over the steps $[1, k]$

$$\begin{aligned}
&\tilde{y}_1 = \tilde{C}_1x_1 + \tilde{D}_1u_1,\\
&\tilde{y}_2 = \tilde{C}_2x_2 + \tilde{D}_2u_2 = \tilde{C}_2(A_1x_1 + B_1u_1) + \tilde{D}_2u_2,\\
&\quad\ldots\\
&\tilde{y}_k = \tilde{C}_k(A_{k-1}\cdots A_1x_1 + A_{k-1}\cdots A_2B_1u_1 + \cdots + B_{k-1}u_{k-1}) + \tilde{D}_ku_k.
\end{aligned} \tag{13}$$

Introduce the notation

$$\begin{aligned}
&\tilde{M}_k = [\tilde{C}_kA_{k-1}\cdots A_1, \tilde{C}_kA_{k-1}\cdots A_2B_1, \tilde{C}_kA_{k-1}\cdots A_3B_2, \ldots, \tilde{C}_kB_{k-1}, \tilde{D}_k],\\
&H_k = \begin{bmatrix} \tilde{M}_1,\ 0_{r\times p(k-1)}\\ \tilde{M}_2,\ 0_{r\times p(k-2)}\\ \ldots\\ \tilde{M}_{k-1},\ 0_{r\times p}\\ \tilde{M}_k \end{bmatrix}, \tilde{Y}_k = \begin{bmatrix} \tilde{y}_1\\ \tilde{y}_2\\ \ldots\\ \tilde{y}_{k-1}\\ \tilde{y}_k \end{bmatrix} = H_kU_k,
\end{aligned} \tag{14}$$

where $0_{r\times p}$ is a zero matrix of the corresponding dimension.

When computing the dynamics of the RS, a recurrent representation of the formulas for computing the matrix relation is also convenient:

$$\begin{aligned}
&M_1 = D_1, H_1 = \tilde{M}_1 = \tilde{D}_1,\\
&M_k = [C_kQ_k, D_k], \tilde{M}_k = [\tilde{C}_kQ_k, \tilde{D}_k], k \in [2, T],\\
&H_k = \begin{bmatrix} H_{k-1},\ 0_{r(k-1)\times p}\\ \tilde{M}_k \end{bmatrix},
\end{aligned} \tag{15}$$

where Q_k is an auxiliary matrix computed iteratively

$$\begin{aligned}
&Q_2 = [A_1, B_1],\\
&Q_k = [A_{k-1}Q_{k-1}, B_{k-1}], k \in [3, T].
\end{aligned} \tag{16}$$

4. SEQUENTIAL ESTIMATION OF THE REACHABILITY SET OVER OUTPUT COMPONENTS

Knowing the matrix relation (12), one can perform a multidimensional estimate of the reachability set. One approach is to divide the reachability set into upper and lower estimates, as shown in [18]. In this splitting, the upper estimate is a hyperrectangle circumscribed around set (7), and the lower estimate is a hypercube centered at the origin inscribed into set (7) in the m-dimensional space. This approach is illustrative; however, in the general case a large gap arises between the upper and lower estimates, leading to considerable uncertainty when estimating the reachability set. This is clearly shown in Fig. 1 for the two-dimensional case.

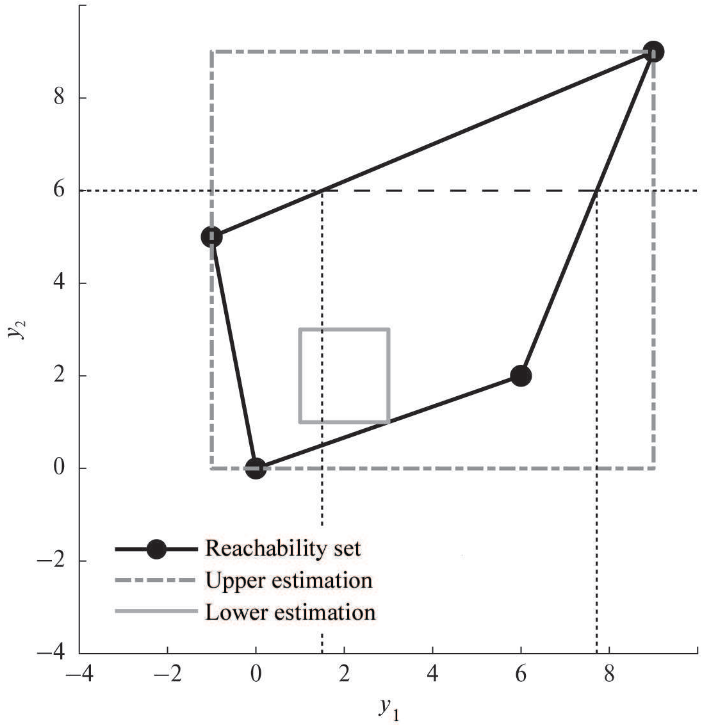

Fig. 1. Illustration of the lower and upper estimates of the reachability set in the two-dimensional case. The dashed line $y_2 = 4$ shows fixing the value of one of the outputs, then the dash-dotted line corresponds to the reachability set with respect to the y_1 coordinate.

A more informative approach can be the sequential finding of an upper estimate followed by fixing the value of one of the outputs within the admissible range, after which a new upper estimate can be found taking into account the fixed output. This procedure can be repeated as many times as there are outputs in the considered system.

Let us consider in more detail the process of constructing a sequential estimate of the reachability set. The first step of the algorithm for finding a sequential estimate of the reachability set is to find an upper estimate of the reachability set over all components of the output vector. This estimate can be found by solving m problems for the maximum

$$\max\{y_T^{(i)} = M_T^{(i)}U_T : \tilde{Y}_T = H_T U_T, x_1 \in X_1, u_k \in P, \tilde{y}_k \in F, k \in [1,T], i \in [1,m]\} \tag{17}$$

and minimum

$$\min\{y_T^{(i)} = M_T^{(i)}U_T : \tilde{Y}_T = H_T U_T, x_1 \in X_1, u_k \in P, \tilde{y}_k \in F, k \in [1,T], i \in [1,m]\}, \tag{18}$$

where $M_k^{(i)}$ is the row of matrix M_k. Problems (17), (18) are linear programming problems that can be solved by the simplex method [15], the interior-point method [20], etc. Generally speaking, the systems of equations (17), (18) may be inconsistent; let us consider the conditions for the existence of a solution.

A solution exists if one of the two statements holds: only constraints on the initial state and controls (3), (4) are given, $r = 0$, or the upper and lower constraints on the initial conditions, controls, and outputs have opposite signs. In the first case, systems (17), (18) always have at least one solution, since there are no constraints on the output signals, and at least one input signal, for example $u_k^{(i)} = u_{\min}^{(i)}$, $i \in [1,n]$, is realizable, and consequently at least one output signal is realizable. In the presence of constraints on a part of the outputs (5) and for $r \neq 0$, a sufficient (but not necessary) condition for the existence of a solution is

$$\begin{cases} x_{\min}^{(i)} \leqslant 0 \leqslant x_{\max}^{(i)}, \ i \in [1, n], \\ u_{\min}^{(i)} \leqslant 0 \leqslant u_{\max}^{(i)}, \ i \in [1, p], \\ \tilde{y}_{\min}^{(i)} \leqslant 0 \leqslant \tilde{y}_{\max}^{(i)}, \ i \in [1, r]. \end{cases} \tag{19}$$

This can be easily verified by substituting the zero vector as the control signal at each step. Such an additional constraint condition is natural for linear systems.

Thus, for each component of the output vector an interval is found in which it can vary $y_{T\ \min\ 1}^{(i)} \leqslant y_T^{(i)} \leqslant y_{T\ \max\ 1}^{(i)}$, $i \in [1, m]$. The user is offered to choose one of the components and fix its value. Without loss of generality, assume that the value of the first component is fixed: $y_T^{(1)} = y^{(1)}$. Consider the second step of the algorithm. To find the upper estimate for the remaining $(m-1)$ components, it is necessary to solve the following problems: for the maximum

$$\begin{cases} y_T^{(1)} = M_T^{(1)} U_T, \\ \max\{y_T^{(i)} = M_T^{(i)} U_T : \tilde{Y}_T = H_T U_T, x_1 \in X_1, u_k \in P, \tilde{y} \in F, k \in [1, T] i \in [2, m]\} \end{cases} \tag{20}$$

and for the minimum

$$\begin{cases} y_T^{(1)} = M_T^{(1)} U_T, \\ \min\{y_T^{(i)} = M_T^{(i)} U_T : \tilde{Y}_T = H_T U_T, x_1 \in X_1, u_k \in P, \tilde{y} \in F, k \in [1, T] i \in [2, m]\}. \end{cases} \tag{21}$$

Thus, at the second step new estimates will be found $y_{T\ \min\ 2}^{(i)} \leqslant y_T^{(i)} \leqslant y_{T\ \max\ 2}^{(i)}$, $i \in [2, m]$. Having performed the remaining steps of the algorithm in a similar way, after m steps, we obtain the problem

$$\begin{cases} y_T = M_T U_T, \\ \tilde{Y}_T = H_T U_T, x_1 \in X_1, u_k \in P, \tilde{y}_k \in F, k \in [1, T], \end{cases} \tag{22}$$

where $y_T \in Y(x_{\min}, x_{\max}, u_{\min}, u_{\max}, \tilde{y}_{\min}, \tilde{y}_{\max}, T)$ is a realizable value of the output vector. Problems (20), (21, (22) are also linear programming problems, and they have a solution because the equality-type constraint on the output signal added at each step is consistent with the other equations, since it satisfies the constraints of the analogous problem at the previous step. The solution to problem (22) is the vector $U_T^* \in \mathbb{R}^{(kp+n)}$, containing the initial conditions $x_1^* \in X_1$ and the open-loop control $u_k^* \in P$, $j \in [1, T]$, realizing the output y_T.

5. EXAMPLE

Let us demonstrate the algorithm on the example considered in [6]. The plant model is:

$$\begin{cases} x_{k+1} = & \begin{bmatrix} 0.8877 & -0.012 \\ 0.0258 & 0.4215 \end{bmatrix} \begin{bmatrix} \cos\frac{\pi}{18}(k-1) & \sin\frac{\pi}{36}(k-1) \\ -\sin\frac{\pi}{36}(k-1) & \cos\frac{\pi}{18}(k-1) \end{bmatrix} x_k + \begin{bmatrix} 1 & 0.5 \\ 0 & 1 \end{bmatrix} u_k; \\ y_k = & \begin{bmatrix} 1 & 0 \\ 0 & 1 \end{bmatrix} x_k; \end{cases} \tag{23}$$

constraints on the control actions and the initial state vector:

$$|x_1^{(1)}| \leqslant 5, \ |x_1^{(2)}| \leqslant 5, \ |u^{(1)}| \leqslant 1, \ |u^{(2)}| \leqslant 1.5. \tag{24}$$

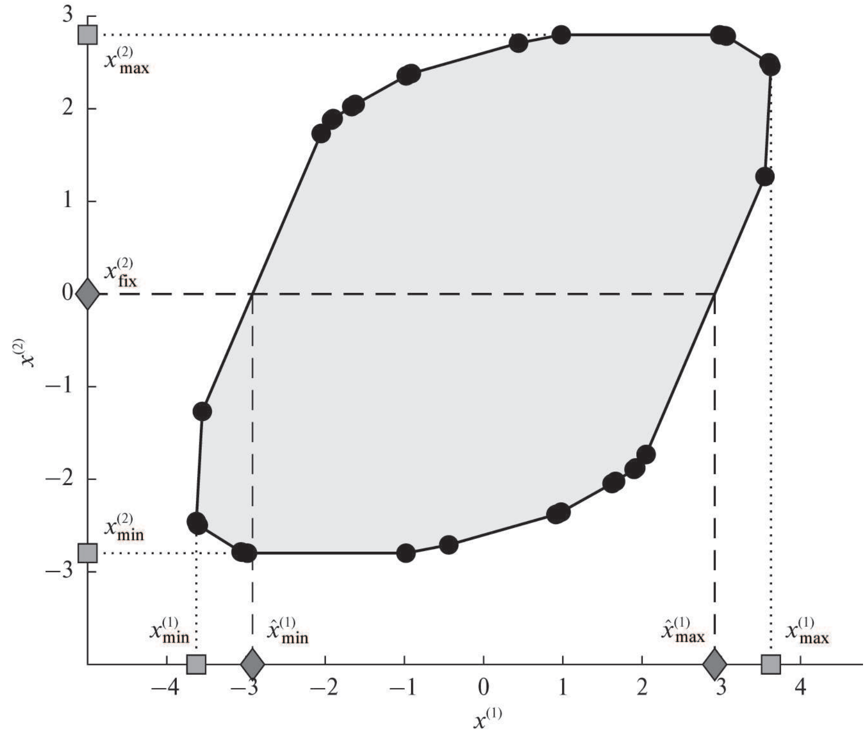

Fig. 2. Reachability set obtained by the method of [6] (dark circles) and by the method described in this paper (squares and diamonds).

In [6] the state reachability set is considered, while in this paper we consider the output reachability set. To enable comparison, in model (23) the output matrix is the identity matrix. Thus, the state vector equals the output vector. In this example there are no constraints on the output signals, $r = 0$. After seventy time steps the state reachability set found by the method of [4, 6] is shown in Fig. 2 with round markers and filling. The algorithm proposed in this paper gives at the first step an estimate of the reachability set over each component: $x^{(i)}_{\rm min} \leqslant x^{(i)} \leqslant x^{(i)}_{\rm max}$, $i \in [1, 2]$, thus obtaining a rectangle circumscribed around the reachability set. The first step of finding the reachability set is shown in Fig. 2 with square markers, $-3.6276 \leqslant x^{(1)} \leqslant 3.6276$, $-2.7982 \leqslant x^{(2)} \leqslant 2.7982$. At the second step the user fixes one of the vector components, for example: $x^{(2)} = x^{(2)}_{\rm fix} = 0$, and the algorithm allows finding the changed estimate of the reachability set over the remaining component of the state vector (which equals the output vector in this example). In Fig. 2 the second step is shown with diamond-shaped markers, $-2.9178 \leqslant x^{(1)} \leqslant 2.9178$. At the final step the user can specify a correct value of the remaining component, and the algorithm will compute one of the possible open-loop controls realizing the obtained output vector at the given time step.

Thus, by successive approximations over each component of the output (state) vector, a point inside the reachability set and an open-loop control realizing the achievement of this point were found.

6. ESTIMATION OF THE REACHABILITY SET FOR THE GLOBUS-M2 TOKAMAK

The method described above for obtaining the reachability set was applied to find possible plasma shape configurations in the Globus-M2 tokamak (Ioffe Institute, St. Petersburg). Linear models with variable parameters and constraints on input and output signals were considered.

6.1. Experimental Signals

In the Globus-M2 tokamak [21, 22] voltages and currents in the control coils are measured, as well as signals from magnetic diagnostic loops during the plasma discharge. The measurement time step is 0.1 ms. The control coils are the central solenoid, the horizontal and vertical field coils, two poloidal field coils, and a correction coil. The magnetic diagnostics consists of twenty-one loops mounted on the vacuum vessel surface and measures the poloidal magnetic flux. Using the coil signals and the magnetic diagnostics, the plasma shape in the divertor discharge phase was reconstructed with the same time step of 0.1 ms [23]. By plasma shape we mean 24 gaps between the tokamak limiter wall and the plasma boundary along directions with a step of 15° (Fig. 3).

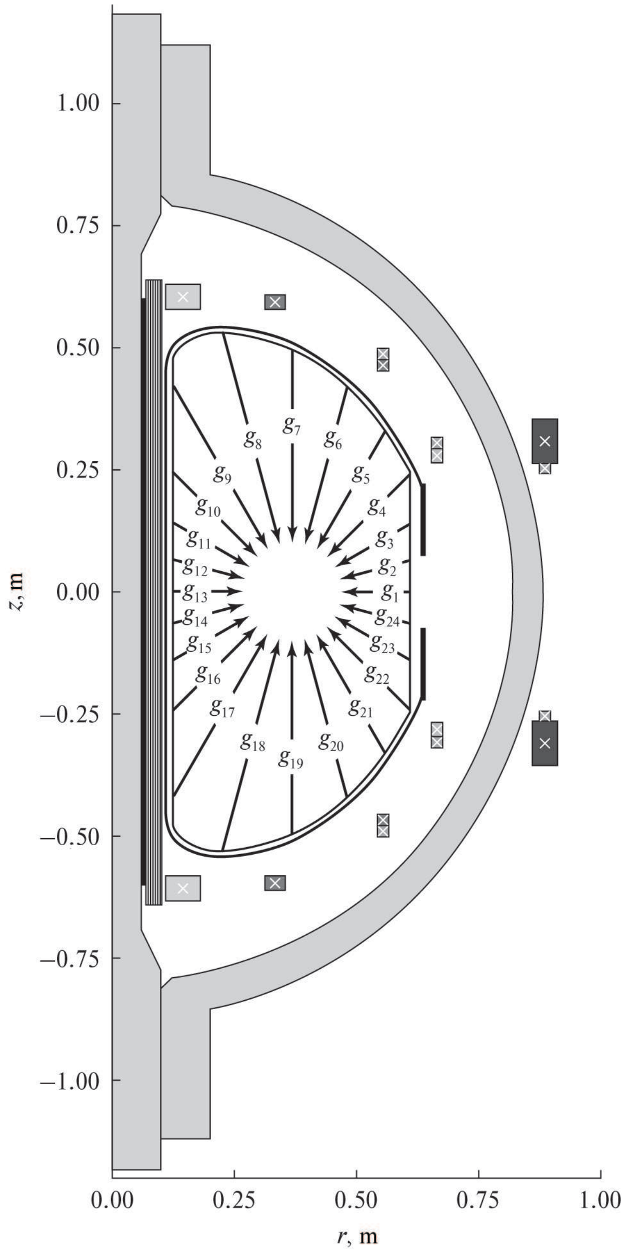

Fig. 3. Vertical cross-section of the Globus-M2 tokamak. Arrows indicate 24 directions along which the 24 gaps g_1–g_{24} between the tokamak limiter and the plasma boundary are measured.

Thus, experimental signals from the control coils were obtained with a 0.1 ms step over the time interval 0.15–0.24 s:

$$U_{PF,\,k} = [U_{HFC,\,k}, U_{VFC,\,k}, U_{CS,\,k}, U_{CC,\,k}, U_{PF1,\,k}, U_{PF3,\,k}]^\top,$$

$$I_{PF\,k} = [I_{HFC,\,k}, I_{VFC,\,k}, I_{CS,\,k}, I_{CC,\,k}, I_{PF1,\,k}, I_{PF3,\,k}]^\top$$

and the gaps between the plasma boundary and the tokamak limiter $G_k = [g_{1,\,k}, \ldots, g_{24,\,k}]^\top$, as well as the vertical position of the plasma column center Z, reconstructed from the magnetic measurements. Hereafter we will refer to these signals as experimental or scenario signals.

6.2. Model

To assess the capability of the tokamak to obtain plasma configurations, its linear model was built. The Globus-M2 tokamak models [12, 13] are constructed from the experimental data of discharges nos. 41 805, 41 835, and 41 867 in deviations from the experimental signals in discrete time with variable parameters:

$$\begin{aligned} x_{k+1} &= A_k x_k + B_k \delta u_k, \\ \delta y_k &= C_k x_k, \\ \delta \tilde{y}_k &= \tilde{C}_k x_k, \end{aligned} \tag{25}$$

where $x \in \mathbb{R}^{17}$, $\delta u = [\delta U_{HFC}, \delta U_{VFC}, \delta U_{CS}, \delta U_{CC}, \delta U_{PF1}, \delta U_{PF3}]^\top \in \mathbb{R}^6$ are deviations from the scenario voltages in the control coils, $\delta y = [\delta g_1, \ldots, \delta g_{24}]^\top \in \mathbb{R}^{24}$ are changes in the shape relative to the scenario signals, $\delta \tilde{y} = [\delta Z, \delta I_{HFC}, \delta I_{VFC}, \delta I_{CS}, \delta I_{CC}, \delta I_{PF1}, \delta I_{PF3}]^\top \in \mathbb{R}^7$ are changes in the vertical plasma position and currents in the control coils. The matrices of the stationary linear models $\hat{A}_i$, $\hat{B}_i$, $\hat{C}_i$ are computed over the time interval from 0.13 to 0.24 s with a step of 1 ms and interpolated linearly:

$$A_k = \frac{10 - (k-1)\%10}{10} \hat{A}_{\lfloor \frac{k-1}{10} \rfloor + 1} + \frac{(k-1)\%10}{10} \hat{A}_{\lfloor \frac{k-1}{10} \rfloor + 2}, \tag{26}$$

where $\lfloor \cdot \rfloor$ denotes rounding down, % is the remainder of division. The matrices B and C are computed analogously.

6.3. Constraints on the Control Signals

Consider deviations from the control signals under the following constraints:

- zero initial conditions $x_1^{(j)} = 0$, $j \in [1, 17]$;
- deviations on the control coil voltages $|\delta u^{(j)}| \leqslant 100$ V, $j \in [1, 6]$;
- deviations on the unstable vertical position of the plasma column center $|\delta Z| \leqslant 1$ cm;
- deviations on the currents in the control coils $|\delta I_{HFC}| \leqslant 500$ A, $|\delta I_{VFC}| \leqslant 500$ A, $|\delta I_{CS}| \leqslant 5$ kA, $|\delta I_{CC}| \leqslant 500$ A, $|\delta I_{PF1}| \leqslant 500$ A, $|\delta I_{PF3}| \leqslant 500$ A.

The voltages in the control coils vary in the range ± 1.6 kV, typical values of currents in the HFC, VFC, CC coils are 0.5 kA, PF1—1.5 kA, PF3—3 kA, the current in the CS coil varies from 0.5 to 2.5 kA. Typical values of the vertical displacement are on the order of 1 cm (Fig. 4). Therefore, one can consider the deviations from the scenario values small and apply linear plasma models for subsequent computations.

Thus, the model equations (25) and the constraints at each step satisfy the problem statement (2), (3), (4), (5) and condition (19). At the same time, the approach to computing the RS described in [4–6] is inapplicable to these models, since it requires constructing the convex hull of points in a space whose dimension equals the number of model states, in this case 17. In such a

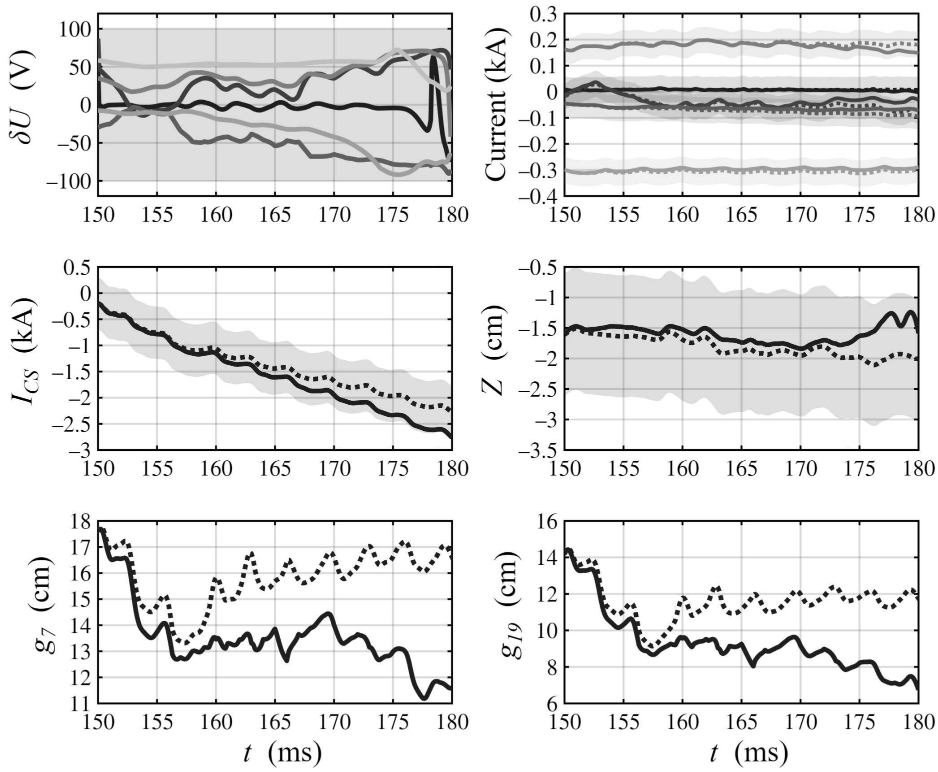

Fig. 4. Simulation result of the plasma with a modified control realizing after 30 ms deviations in the shape components $\delta g_7 = -5$ cm, $\delta g_{19} = -5$ cm, additionally elongating the plasma vertically under constraints on the vertical plasma displacement, voltages and currents in the control coils. Dashed lines—scenario, solid lines—deviated signals, halftone—admissible deviations. Discharge no. 41 805.

space the points form a d-polytope having at least $N = 2^d$ vertices, according to (1) $F(d) \sim 2^{3d/2}$ hyperfaces, and at each step this number increases proportionally to the number of inputs. Thus, the method described in Sections 2, 3, 4 becomes relevant.

6.4. Plasma Shape Reachability Set

Let us analyze the possibility of changing the shape components g_7 and g_{19}—the upper and lower points of the plasma. By changing these quantities one can influence the plasma vertical elongation. Decreasing the gaps between the plasma and the vacuum vessel wall corresponds to increasing elongation. The initial value of the state vector is assumed to be zero.

Using the proposed algorithm, we obtain for the model of discharge no. 41 805 that after 30 ms (300 time steps) the system outputs δg_7 and δg_{19} are constrained within the intervals:

$$-7.9 \leqslant \delta g_7 \leqslant 7.9; \ -8.6 \leqslant \delta g_{19} \leqslant 8.6, \tag{27}$$

where the deviation values are expressed in centimeters. At the second step we fix $\delta g_7 = -5.0$ cm, then we obtain:

$$\delta g_7 = -5.0; \ -8.6 \leqslant \delta g_{19} \leqslant -2.9. \tag{28}$$

At the last step we can fix the value $\delta g_{19} = -5.0$ cm and obtain an open-loop control, the output deviation values of 5 cm. The dynamics of the system with the found open-loop control are shown in Fig. 4.

Thus, it is shown that using the poloidal field coils it is possible to increase the vertical elongation of the plasma in the existing configuration of the Globus-M2 tokamak.

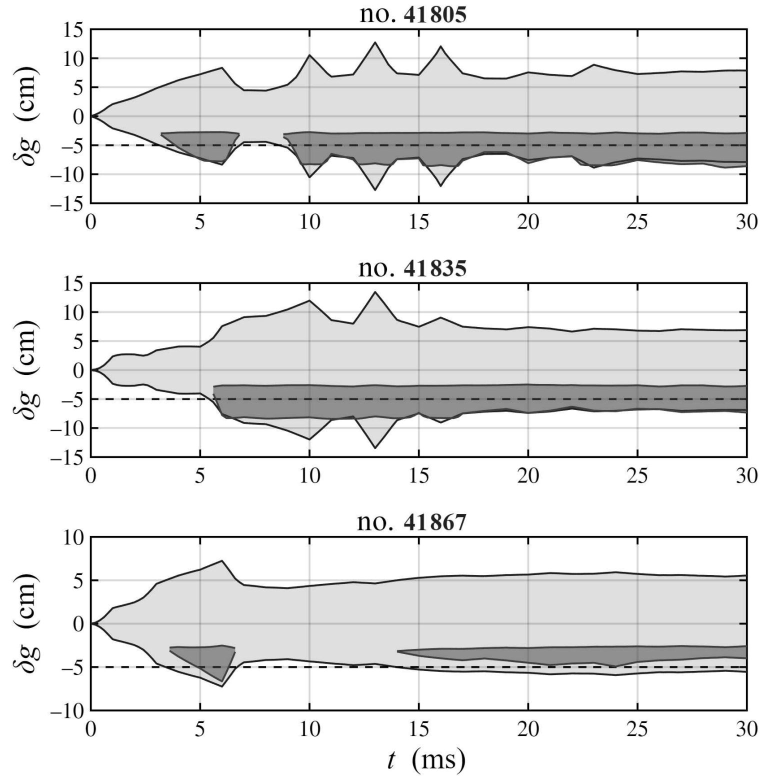

Fig. 5. Change in the reachability set during the divertor discharge phase. Light gray shows the reachability set with respect to the deviation for the gap δg_7, dark gray—for the gap δg_{19}, under the condition $\delta g_7 = -5$ cm, at those time instants where such a condition is feasible. Time is given from the start of the divertor phase.

Let us analyze the change in the reachability sets over these shape components with time. Consider plasma discharges no. 41 805, 41 835, 41 867. Compute the possible deviation in δg_7. If the deviation in δg_7 can be equal to -5 cm, we fix it and find the reachability set with respect to δg_{19}. The result is shown in Fig. 5, the time is given from the beginning of the divertor phase. A strong coupling between the opposite gaps is visible; a deviation of the δg_7 component inevitably leads to a deviation of the δg_{19} component in the same direction.

7. CONCLUSION

The paper proposes a method for finding points lying inside a multidimensional reachability set for linear discrete-time systems with variable parameters. A computationally efficient algorithm has been developed that allows sequentially estimating cross-sections of the reachability set over the output vector components, finding points inside the RS using linear programming problems. The method has been applied to the plasma control problem in the Globus-M2 tokamak, which made it possible to find attainable plasma configurations under given control constraints, to demonstrate the possibility of increasing the vertical elongation of the plasma, and to analyze the change in the RS during the plasma discharge. The numerical experiments performed demonstrate consistency of the results with known methods for low-dimensional cases, practical applicability of the approach for systems with dozens of state variables, and the ability to account for variable parameters.

The proposed approach opens new possibilities for analysis and synthesis of control systems for complex dynamic plants, where traditional methods for constructing the RS become inapplicable due to high computational complexity. The developed algorithm can be useful both for theoretical studies of controllability properties of dynamical systems and for solving applied control problems for complex engineering objects.

ACKNOWLEDGMENTS

The author thanks the Globus-M2 tokamak team for the experimental data provided, and P.S. Korenev for the plasma models provided.

FUNDING

This work was supported by the Russian Science Foundation, grant no. 21-79-20180-P, https://rscf.ru/project/21-79-20180/.

REFERENCES

1. Polyak, B.T., Khlebnikov, M.V., and Shcherbakov, P.S., *Upravlenie lineinymi sistemami pri vneshnikh vozmushcheniyakh (tekhnika lineinykh matrichnykh neravenstv)* (Control of Linear Systems under External Disturbances. Linear Matrix Inequality Technique), Moscow: LENAND, 2014.

2. Krasovskii, N.N., *Teoriya upravleniya dvizheniem* (Theory of Motion Control), Moscow: Nauka, 1968.

3. Afanas'ev, V.N., *Teoriya optimal'nogo upravleniya nepreryvnymi dinamicheskimi sistemami. Analiticheskoe konstruirovanie* (Theory of Optimal Control of Continuous Dynamical Systems. Analytical Design), Moscow: Publishing House of the Physical Faculty of Moscow State University, 2011.

4. Tyulyukin, V.A. and Shorikov, A.F., An Algorithm for Solving a Terminal Control Problem for a Linear Discrete System, *Avtomat. i Telemekh.*, 1993, no. 4, pp. 115–127; *Autom. Remote Control*, 1993, vol. 54, no. 4, pp. 632–643.

5. Bulaev, V.V. and Shorikov, A.F., Modification of the General Recurrent Algebraic Method for Constructing Reachability Domains of Linear Discrete Controlled Systems, *Informatsionnye tekhnologii i sistemy: Trudy Shestoi Mezhdunarodnoi nauchnoi konferentsii* (Information Technologies and Systems: Proc. Sixth Int. Sci. Conf.), 2017, pp. 47–52.

6. Bulaev, V.V. and Osipov, I.O., Modified Algorithm for Constructing Reachability Domains of Linear Discrete Dynamical Systems, *Vestn. Yuzhno-Ural. Gos. Univ. Ser. Komp. Tekhnol., Upravl., Radioelektron.*, 2018, vol. 18, no. 1, pp. 56–62.

7. Shcherbakov, P.S., Reachability Sets of Linear Systems: Definitions, Basic Properties, Approximations, *Trudy 11-i Vserossiiskoi shkoly-konferentsii molodykh uchenykh UBS* (Proc. 11th All-Russian School-Conf. Young Scientists UBS), 2014, pp. 15–19.

8. Khlebnikov, M.V., Outer Estimate of the Reachability Set of a Linear Dynamical System, *Stokhasticheskaya optimizatsiya v informatike*, 2016, vol. 12, pp. 112–122.

9. Preparata, F.P. and Shamos, M.I., *Computational Geometry: An Introduction*, New York: Springer, 1985.

10. Klee, V., Convex Polytopes and Linear Programming, *Proc. IBM Sci. Comput. Symp. Combinatorial Problems*, IBM, White Plains, USA, 1966, pp. 123–158.

11. Balashov, M.V. and Tremba, A.A., Some Set-Theoretic Operations with the Reachability Set of a Linear Controlled System, *Materialy Mezhdunarodnoi konferentsii "Differentsial'nye uravneniya i optimal'noe upravlenie", posvyashchennoi 100-letiyu so dnya rozhdeniya akademika E.F. Mishchenko* (Proc. Int. Conf. "Differential Equations and Optimal Control" Dedicated to the 100th Anniversary of Academician E.F. Mishchenko), 2022, pp. 20–22.

12. Korenev, P.S., Mitrishkin, Yu.V., and Patrov, M.I., Reconstruction of the Equilibrium Distribution of Tokamak Plasma Parameters from External Magnetic Measurements and Construction of Linear Plasma Models, *Mekhatronika, Avtomatizatsiya, Upravlenie*, 2016, vol. 17, no. 4, pp. 254–265.

13. Konkov, A.E., Korenev, P.S., Mitrishkin, Yu.V., et al., Real-Time Magnetic Plasma Control System with Equilibrium Reconstruction Algorithm in Feedback for the Globus-M2 Tokamak, *Fizika Plazmy*, 2023, vol. 49, no. 12, pp. 1348–1356.

14. Korenev, P.S., Konkov, A.E., Chektybaev, B.Zh., et al., Estimation of the Vertical Plasma Position Controllability Region in the KTM Tokamak with HFC Coil, *VANT. Ser. Termoyadernyi sintez*, 2024, vol. 47, no. 3, pp. 49–59.

15. Karmanov, V.G., *Matematicheskoe programmirovanie* (Mathematical Programming), 5th ed., Moscow: FIZMATLIT, 2024.

16. Yudin, D.B. and Golshtein, E.G., *Zadachi i metody lineinogo programmirovaniya* (Problems and Methods of Linear Programming), Moscow: Sov. Radio, 1964.

17. Borgwardt, K., *The Simplex Method: A Probabilistic Analysis* (Algorithms and Combinatorics, Study and Research Texts), Berlin: Springer-Verlag, 1987.

18. Mitrishkin, Y.V., Kruzhkov, V.I., and Korenev, P.S., Methodology of Plasma Shape Reachability Area Estimation in D-Shaped Tokamaks, *Mathematics (MDPI)*, 2022, no. 10(23).

19. Mitrishkin, Y.V., Kruzhkov, V.I., and Patrov, M.I., Estimation of Controllability Region of Unstable Vertical Plasma Position and Plasma Separatrix Multivariable Reachability Area of a Spherical Tokamak. EPS2019, *Proc. 46th European Physical Society Conf. on Plasma Physics*, Milan: European Physical Society, 2019, pp. 4.1095.

20. Dikin, I.I., Iterative Solution of Linear and Quadratic Programming Problems, *Dokl. Akad. Nauk SSSR*, 1967, vol. 174, no. 4, pp. 747–748.

21. Minaev, V.B., Gusev, V.K., Sakharov, N.V., et al., Spherical Tokamak Globus-M2: Design, Integration, Construction, *Nuclear Fusion*, 2017, vol. 57, pp. 066047.

22. Mitrishkin, Y.V., Korenev, P.S., Prokhorov, A.A., et al., Plasma Control in Tokamaks. Part 1. Controlled Thermonuclear Fusion Problem. Tokamaks. Components of Control Systems, *Advanc. Syst. Sci. Appl.*, 2018, vol. 18, no. 2, pp. 26–52.

23. Korenev, P.S., Konkov, A.E., Mitrishkin, Yu.V., et al., Improved FCDI algorithm for tokamak plasma equilibrium reconstruction, *Technical Physics Letters*, 2023, vol. 49, no 4. pp. 34–37.

This paper was recommended for publication by M.V. Khlebnikov, a member of the Editorial Board